Journal of Process Control 24 (2014) 341–347

Contents lists available at ScienceDirect

Journal of Process Control

journal homepage: www.elsevier.com/locate/jprocont

Analysis of a synthetic gene switching motif: Systems and control approaches☆

Kwang-Ki K. Kim[a,b], Kim Seng Cheong[a,d], Kejia Chen[a], Richard D. Braatz[c,*]

[a] University of Illinois at Urbana-Champaign, Urbana, IL, USA
[b] Georgia Institute of Technology, Atlanta, GA, USA
[c] Massachusetts Institute of Technology, Cambridge, MA, USA
[d] National University of Singapore, Singapore

ARTICLE INFO

Article history:
Received 28 December 2012
Received in revised form 3 December 2013
Accepted 7 December 2013
Available online 5 February 2014

Keywords:
Performance analysis
Stability analysis
Stochastic stability
Sensitivity analysis
Systems biology

ABSTRACT

Developing predictive mathematical models for regulatory networks in biological systems would be useful for their analysis and design. This paper studies the parameter-dependent characteristics of a gene switching model that consists of dual positive feedback loops. Deterministic and stochastic stability are studied for this model, as well as other important system behaviors such as convergence rate to a stable equilibrium point, hysteresis induced by two time scales of the system model, and noise sensitivity with respect to the system parameters. Sensitivity of system performance indices with respect to the system parameters are analyzed in terms of $\mathcal{H}_\infty$- and $\mathcal{H}_2$-norms of the linearized system model with their closed-form solutions. The presented qualitative and quantitative studies of the system characteristics enable the synthesis of a robust gene regulatory network that achieves desired static and dynamic responses.

1. Introduction

The development of predictive mathematical models of regulatory networks in living cells could revolutionize the study of complex diseases. Progress in the development of such mathematical models has been limited by both the incompleteness of the experimental data and the high complexity of the networks, which has motivated many researchers to take a 'coarse-grained' approach, in which the mathematical models are developed to describe the dynamical systems behavior without attempting to describe all of the molecular details [1,2]. This approach has been applied to gain insights into regulatory and signaling behavior for a wide variety of biological regulatory networks including those associated with mammalian circadian rhythm [3], the yeast cell-cycle network [4], folding pathways in yeast [5], macrophages [6], neutrophils [7], and somitogenesis oscillation in zebrafish [8,9].

Much of the research efforts have been in the identification of functional motifs that are connected to form larger regulatory networks [2,7,10–15]. These motifs include switches, oscillators, biphasic amplitude filters, bandpass frequency filters, memory, noise filters, and noise amplifiers [16]. Motifs are especially relevant in synthetic biology, as well-characterized motifs can serve as a basis for the design of a synthetic genetic network to produce a desired dynamic behavior [17]. Successful implementations of this motif-based approach is the design and construction of synthetic gene regulatory networks for toggle switches [18–20], and oscillators with tunable parameters [21–23]. By coupling to cell–cell communication, such motifs have been used to implement built-in regulation of the cell population density in response to changes in the environment [24].

Several researchers have characterized the dynamics of certain classes of these motifs [25], to assist synthetic biologists in their selection and the design of regulatory pathways. Quantitative relationships between the model parameters within a mathematical model of a motif and the dynamics can facilitate both the selection of parameters to obtain a desired regulatory network behavior, as well as the identification of parameters from experimental data where the mathematical model of a motif is used a coarse-grained model of a more complex regulatory network.

This paper characterizes the dynamics of a motif consisting of interlinked fast and slow positive feedback loops, which regulate polarization of budding yeast, calcium signaling, Xenopus oocyte maturation, and other processes [2]. Interest in this motif as a component in synthetic genetic networks is that it provides a dual-time

☆ A preliminary version of part of this manuscript was published as K.-K. Kim, K.S. Cheong, K. Chen, and R.D. Braatz, Parameter estimation, analysis, and design of synthetic gene switching models: System behavior- and performance-based approaches, *Proceedings of the 8th IFAC International Symposium on Advanced Control of Chemical Processes*, Singapore, pp. 946–951, 2012.

* Corresponding author. Tel.: +1 617 253 3112; fax: +1 617 258 5766.
E-mail address: braatz@mit.edu (R.D. Braatz).

0959-1524/$ – see front matter © 2014 Elsevier Ltd. All rights reserved.
http://dx.doi.org/10.1016/j.jprocont.2013.12.004

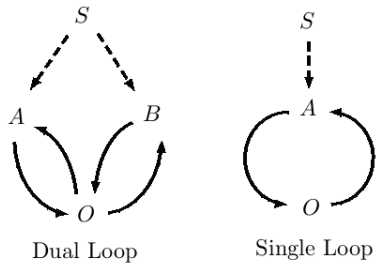

Fig. 1. Structures of feedforward and feedback activations of dual and single loop motifs [2]. The solid lines show feedback relationships between components within the system and the dashed lines show feedforward relationships between the stimulus and the components.

switch that can be rapidly and reliably induced while being relatively insensitive to noise in the stimulus [2]. The control-theoretic point of view on the gene switching model provides information that can be used to design robust biological circuit design of gene switches that perform programmed desired behaviors in the presence of intrinsic and extrinsic perturbations.[1]

1.1. Notation

$\mathbb{R}$ denotes the field of real numbers and $\mathbb{R}_+$ is the set of nonnegative real numbers; $\mathbb{R}^n$ defines a topology on the product of n copies of $\mathbb{R}$; **Pr** is the symbol of the probability; **E** or $\overline{(\cdot)}$ is the symbol of the mathematical expectation or mean; **Var** or $\Sigma_{(\cdot)}$ is the symbol of the mathematical variance or covariance; $\mathcal{N}(a, b)$ is the Gaussian distribution with the mean a and the variance b; the symbol $\sim$ means "distributed as"; $0_{n\times m} \in \mathbb{R}^{n\times m}$ denotes the null matrix whose elements are all zeros; $I_n \in \mathbb{R}^{n\times n}$ denotes the identity matrix. For a square matrix $A \in \mathbb{C}^{n\times n}$, $\sigma(A)$ denotes the set of its eigenvalues.

2. Motif characterization

This section characterizes the dynamics of the motif, including the relationship between the system model parameters and the output. The goal is to understand the general parameter-dependent characteristics of the dynamics of the motif (Fig. 1).

2.1. Mathematical models

Consider the mathematical model for the dual-positive feedback loops motif[2]

$$\begin{aligned}\frac{dA}{dt} &= \tau_a\left(k_{\min} - A + \frac{O^n}{O^n + \mathrm{ec}_{50}}(1-A)S\right)\\ \frac{dB}{dt} &= \tau_b\left(k_{\min} - B + \frac{O^n}{O^n + \mathrm{ec}_{50}}(1-B)S\right)\\ \frac{dO}{dt} &= k_{\mathrm{on}}^{\mathrm{out}}(A+B)(1-O) - k_{\mathrm{off}}^{\mathrm{out}}O + k_{\min}^{\mathrm{out}},\end{aligned} \tag{1}$$

which has been normalized and nondimensionalized. The variables O, A, and B are concentrations between 0 and 1. O is activated by A and B, and a nonlinear Hill function $h(O) \triangleq O^n/(O^n + \mathrm{ec}_{50})$ characterizes the relationship between the concentration of O and the rate of production of A and B. The Hill coefficient is n and the concentration for half-maximum response for the feedback is ec_{50}. The mutual activations O linked together with A and B form the dual positive feedback loops. A and B are also activated by an external stimulus S. The motif dynamics when one of the inner loops is suppressed is also of interest:

$$\begin{aligned}\frac{dA}{dt} &= \tau_a\left(k_{\min} - A + \frac{O^n}{O^n + \mathrm{ec}_{50}}(1-A)S\right)\\ \frac{dO}{dt} &= k_{\mathrm{on}}^{\mathrm{out}}A(1-O) - k_{\mathrm{off}}^{\mathrm{out}}O + k_{\min}^{\mathrm{out}}\end{aligned} \tag{2}$$

where A represents either the fast or the slow loop.

3. System stability analysis

First consider the deterministic stability of the gene switching model (1) for which any intrinsic or extrinsic biochemical noise is ignored so that there is no source of stochasticity. Suppose that all the system parameters are positive. For the switch-off case ($S=0$), its stability is straightforward. The inner-loop dynamics for A and B are linear and globally exponentially stable, and there is no positive feedback from the output O to the inner-loop states A and B. We also have $dO/dt \le -cO + d$ for some constants c, $d > 0$ satisfying $d/c = O_{\mathrm{ss}}$, provided that the initial values of A and B are nonnegative. Therefore, the overall system is semi-global exponentially stable when the initial condition satisfies $(A(0), B(0), O(0)) \in \mathbb{R}^3_+$, which follows from the comparison lemma ([26], Lem. 3.4). For the switch-on case ($S=1$), the inner-loop dynamics for A and B have nonlinear terms, $h(O)(1-A)$ and $h(O)(1-B)$. The property of the Hill function that $0 \le h(O) \le 1$ for all $O \ge 0$ implies that $dA/dt \le \tau_a(-A + k_{\min} + c_A)$ and $dB/dt \le \tau_b(-B + k_{\min} + c_B)$ where the constants c_A and c_B satisfy the relations $k_{\min} + c_A = A_{\mathrm{ss}}$ and $k_{\min} + c_B = B_{\mathrm{ss}}$, respectively. Similar to the switch-off case, there exist constants c, $d > 0$ such that $dO/dt \le -cO + d$ and $d/c = O_{\mathrm{ss}}$, provided $(A(0), B(0)) \in \mathbb{R}^2_+$. Combining those upper bounds and applying the comparison lemma implies that the overall system is semi-global exponentially stable for the initial condition $(A(0), B(0), O(0)) \in \mathbb{R}^3_+$. It is easy to show that, for any positive system parameters, the nonnegative quadrant is a region of attraction to a unique equilibrium point for each case $S=0$ or $S=1$, and is a positively invariant set, i.e., once the solution trajectory enters the nonnegative quadrant, then it will stay inside the nonnegative quadrant for the entire future time and converge to a unique equilibrium point.

Now consider intrinsic and extrinsic biochemical noise in the gene switching model (1). To study the stochastic stability properties of the system model, consider extrinsic noise in the stimulus S and in propagation of inner loop states A and B to the output. More precisely, the system dynamics change according to the stochastic differential equation (SDE):

$$\begin{aligned}\frac{dA}{dt} &= \tau_a\left(k_{\min} - A + \frac{O^n}{O^n + \mathrm{ec}_{50}}(1-A)(S+w_a)\right)\\ \frac{dB}{dt} &= \tau_b\left(k_{\min} - B + \frac{O^n}{O^n + \mathrm{ec}_{50}}(1-B)(S+w_b)\right)\\ \frac{dO}{dt} &= k_{\mathrm{on}}^{\mathrm{out}}(A + v_a + B + v_b)(1-O) - k_{\mathrm{off}}^{\mathrm{out}}O + k_{\min}^{\mathrm{out}},\end{aligned} \tag{3}$$

where $[w_a, w_b, v_a, v_b]^{\mathrm{T}}$ are jointly Gaussian random processes. This ordinary differential equation can be written as $\dot{X} \triangleq dX/dt = F(X) + G(X)W_t$ where $X \triangleq [A, B, O]^{\mathrm{T}}$, $W \triangleq [w_a, w_b, v_a, v_b]^{\mathrm{T}}$, and the nonlinear functions $F : \mathcal{X} \to \mathbb{R}^3$ and $G : \mathcal{X} \to \mathbb{R}^{3\times 4}$ are appropriately defined with the support $\mathcal{X} \subset \mathbb{R}^3_+$ of the state X. Previously we showed that the system $\dot{X} = F(X)$ is deterministically semi-globally exponentially stable for all $X \in \mathbb{R}^3_+$. From a converse Lyapunov theorem (see [26], Thm. 4.17, for example), there exists a smooth positive

[1] In this paper, the term "robustness" is used to refer to any type of resistance or insensitivity against perturbations and unknowns, while performing desired or programmed functions.

[2] See [2] for details in the use of the system model (1) to represent interlinked positive feedback loops in biological regulation.

definite function $V(X)$ defined for all X that satisfies the inequalities

$$\frac{d}{dt}V(\delta X) \le -\alpha V(\delta X), \quad \left\|\frac{\partial V}{\partial X}(\delta X)\right\| \le \beta\|\delta X\|, \quad \left\|\frac{\partial^2 V}{\partial X^2}(\delta X)\right\| \le \gamma,$$

where α, β, $\gamma > 0$ are some constants and $\delta X \triangleq X - X_{ss}$ refers to the deviation from the unique equilibrium point X_{ss}. This result follows from the fact that the Jacobian $\frac{dF}{dX}$ is bounded for all $X \in \mathcal{X} \subset \mathbb{R}^3_+$. The results in ([27], Lem. 9), taking into account the fact that the nonlinear functions F and G satisfy the regularity conditions for the Cauchy problem (see [28], for details), imply that there exists a unique probability density function (pdf) p^* such that the pdf of the solution for the SDE (3) converges to p^*. This implies stochastic asymptotic stability of the solution for the SDE (3) in the presence of non-vanishing stochastic noise W_t.[3]

4. System behavior

4.1. Convergence rate

For a uniform time-scale dynamical system, the convergence rate (or response time) to a stable equilibrium point or an attracting limit cycle is governed by the eigenvalues of the eigenmodes corresponding to the slow dynamics. The case of dual-positive feedback loops motif (1), however, corresponds to a two time-scale dynamical system in which the fast inner-loop dynamics has much smaller time constant, compared to time constant of the slow inner-loop dynamics. There are two distinct stages of system behavior and response to the input. For the switch-on ($S = 1$) case, behavior of the first stage is governed by the fast inner-loop dynamics and the solution trajectory reaches near the stable equilibrium point quickly during this stage, and the last of the dynamic behavior is governed by the slow inner-loop dynamics for which the differential equation corresponding to the fast inner-loop dynamics can be replaced by an algebraic equation and the linearized system provides necessary information about the system during this stage of response. For the switch-off ($S = 0$) case, similarly, behavior of the first stage is governed by the fast inner-loop dynamics, but the solution trajectory is far away from the new stable equilibrium point and the last dynamic behavior is governed by the slow inner-loop dynamics for which the differential equation corresponding to the fast inner-loop dynamics can be also replaced by an algebraic equation. These phenomena are observed in a simulation in Fig. 2 in which hysteresis curves with different values of time constants are provided and an appropriately scaled ramp input instead of the jump stimulus is applied to give clear comparisons between curves.

4.2. Hysteresis

The lag in the responses in Fig. 2 to stimulus (or input) is related to robustness against noise perturbation. As stated in the previous section, most of the time history of the solution trajectory is governed by a slow inner-loop dynamics, and the fast inner-loop dynamics has effects on the system behavior during the first short time period. Qualitatively, the overall system would be expected to be robust against additive noise perturbation in stimulus to the network motif for long time, when the system acts as a low-pass filter, while being sensitive to noise perturbation in short time.

An example hysteresis curve for the dual-positive feedback loops motif is shown in Fig. 3, for the time constants ($\tau_a = 0.5$, $\tau_b = 0.008$). The shape of the hysteresis curves is related to the Hill coefficient. The duration for which the system is governed by the fast inner-loop dynamics is proportional to the Hill coefficient n and the shape of a hysteresis curve is closer to a rectangular box as n increases, when the Hill function becomes steeper (figure not shown due to space constraints).

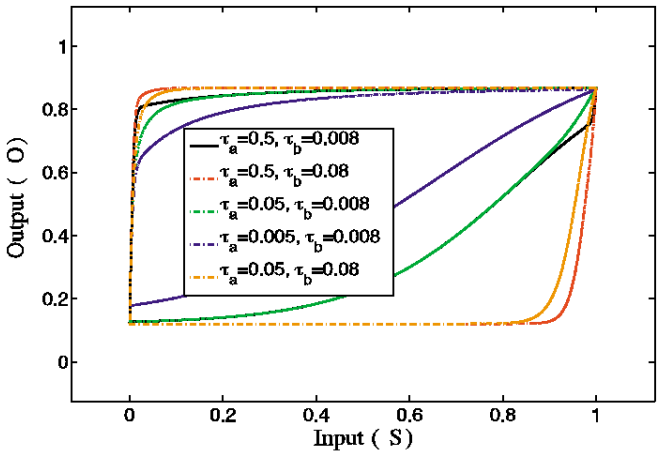

Fig. 2. Hysteresis curves of different time constants.

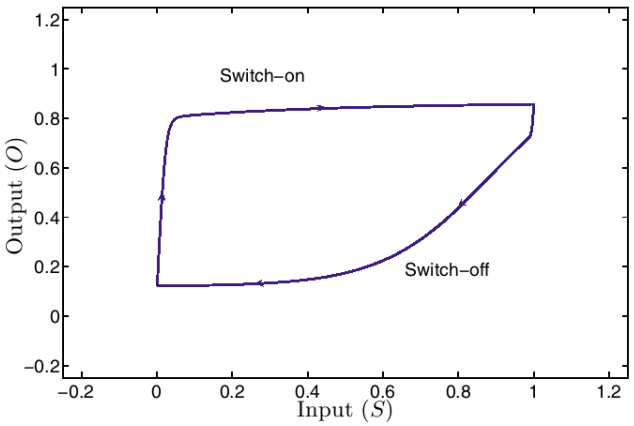

Fig. 3. A hysteresis curve.

4.3. Noise sensitivity

Consider noise perturbation w_t in the stimulus S and assume that the random process w_t is a Wiener process. Consider the case where $S = 1$, since $S = 0$ would imply no signal exchange for which no perturbation will propagate. To investigate the effect of this noise perturbation on the solution trajectory or the system output, first define a probability space. Let Ω be a sample space equipped with a σ-algebra $\mathcal{F}$. Consider a probability measure μ that is defined on $(\Omega, \mathcal{F})$ and the corresponding probability (measure) space defined by $(\Omega, \mathcal{F}, \mu)$. The underlying probability space and measure are determined by the primitive random variables or processes.

Setting $S = 1$, consider an autonomous stochastic differential equation (SDE)

$$dx = f(x)dt + g(x)dw_t \tag{4}$$

where $x = [A, B]^T$,

$$f(x) = \begin{bmatrix} \tau_a\,(k_{\min} - (1 + h(O))A + h(O)) \\ \tau_b\,(k_{\min} - (1 + h(O))B + h(O)) \end{bmatrix},$$

[3] In this system, the noise perturbation is persistent due to $G(X_{ss}) \neq 0$, which implies that the noise perturbation does not vanish even when $X = X_{ss}$.

and

$$g(x) = \begin{bmatrix} \tau_a h(O)(1-A) \\ \tau_b h(O)(1-B) \end{bmatrix}.$$

The goal is to study the probability density function of the solution x_t, denoted by $p(x, t; x_0, t_0)$ with the initial condition $x_0 = x(t_0)$, and its sensitivity with respect to the system parameters. The Fokker–Planck equation (aka the Kolmogorov forward equation) can be used for computing the probability density for this stochastic process. The associated problem is called the *Cauchy problem* in the partial differential equation literature, which usually does not have a closed-form solution and can be hard to solve numerically for general systems. To study the parameter sensitivity, instead of solving the Fokker–Planck equation to compute the evolution of the probability distribution of x_t, this paper uses the linearized model of the motif dynamics (1):

$$\frac{dX}{dt} = \mathcal{A}X + \mathcal{B}w; \quad Y = \mathcal{C}X \tag{5}$$

where $X \triangleq [\delta A, \delta B, \delta O]^{\mathrm{T}}$ denotes the deviation of the steady-state and the system matrices are

$$\mathcal{A} = \begin{bmatrix} -\tau_a(1+h(y)u) & 0 & \tau_a(1-x_1)h'(y)u \\ 0 & -\tau_b(1+h(y)u) & \tau_b(1-x_1)h'(y)u \\ k_{\mathrm{on}}^{\mathrm{out}}(1-x_3) & k_{\mathrm{on}}^{\mathrm{out}}(1-x_3) & \begin{pmatrix} -k_{\mathrm{on}}^{\mathrm{out}}(x_1+x_2) \\ -k_{\mathrm{off}}^{\mathrm{out}} \end{pmatrix} \end{bmatrix},$$

$$\mathcal{B} = [(1-x_1)h(y) \quad (1-x_2)h(y) \quad 0]^{\mathrm{T}}, \mathcal{C} = [0 \quad 0 \quad 1];$$

$h(y) \triangleq \frac{y^n}{y^n + \mathrm{ec}_{50}^n}$, $h'(y) \triangleq \frac{dh(y)}{dy} = \frac{ny^{n-1}\mathrm{ec}_{50}^n}{(y^n+\mathrm{ec}_{50}^n)^2}$, $x_1 = x_2 = A_{\mathrm{ss}} = B_{\mathrm{ss}}$, $y = x_3 = O_{\mathrm{ss}}$, and $u = S_{\mathrm{ss}}$. For a Gaussian white noise w_t with the statistics $\mathbf{E}[w_t] = 0$ and $\mathbf{E}[w_t w_s^{\mathrm{T}}] = \delta(t-s)\Sigma_w$, the solution trajectory of (5) is a Gaussian random process and its mean $\overline{X}_t$ and covariance $\Sigma_{X,t}$ solve the linear system equations

$$\begin{aligned} \frac{d\overline{X}}{dt} &= \mathcal{A}\overline{X}; \overline{X}_0 = \mathbf{E}[X_0] \\ \frac{d\Sigma_X}{dt} &= \Sigma_X\mathcal{A} + \mathcal{A}^{\mathrm{T}}\Sigma_X + 2\mathcal{B}\Sigma_w\mathcal{B}^{\mathrm{T}}; \Sigma_{X,0} = \mathbf{E}[X_0X_0^{\mathrm{T}}] \end{aligned} \tag{6}$$

and the system output is also a Gaussian random process, $Y_t \sim \mathcal{N}(\overline{Y}_t, \Sigma_{Y,t})$, where $\overline{Y}_t = \mathcal{C}\overline{X}_t$ and $\Sigma_{Y,t} = \mathcal{C}\Sigma_{X,t}\mathcal{C}^{\mathrm{T}}$. The analysis goal is to quantify the sensitivity of $\Sigma_{Y,t} \in \mathbb{R}_+$ with respect to the system parameters. In particular, consider the system parameters $\{\tau_a, \tau_b, k_{\mathrm{on}}^{\mathrm{out}}, k_{\mathrm{off}}^{\mathrm{out}}\}$, the steady-state solution $\Sigma_{X,\mathrm{ss}}$ for the second dynamic system in (6), i.e., $\Sigma_{X,\mathrm{ss}}$ satisfying the linear (Lyapunov) equation

$$\Sigma_{X,\mathrm{ss}}\mathcal{A} + \mathcal{A}^{\mathrm{T}}\Sigma_{X,\mathrm{ss}} + 2\mathcal{B}\Sigma_w\mathcal{B}^{\mathrm{T}} = 0 \tag{7}$$

and the corresponding steady-state of the output covariance $\Sigma_{Y,\mathrm{ss}} = \mathcal{C}\Sigma_{X,\mathrm{ss}}\mathcal{C}^{\mathrm{T}}$. A solution for the Lyapunov equation (7) exists if and only if the matrix $\mathcal{A}$ is Hurwitz stable, i.e., $\sigma(\mathcal{A}) \subset \mathbb{C}_-$, and is unique if and only if the pair $(\mathcal{A}, \mathcal{B}\Sigma_w^{1/2})$ is controllable.

To analyze the sensitivity of the Lyapunov solution $\Sigma_{X,\mathrm{ss}}$ with respect to the variation of the system parameters $\{\tau_a, \tau_b, k_{\mathrm{on}}^{\mathrm{out}}, k_{\mathrm{off}}^{\mathrm{out}}\}$, consider a variation in the matrix $\mathcal{A}$, denoted by $\delta\mathcal{A}$, such that the perturbed system matrix is $\hat{\mathcal{A}} = \mathcal{A} + \delta\mathcal{A}$. This notation of variation can be used to represent the parametric perturbation in the linearized motif dynamics (5) due to the linear dependence of $\mathcal{A}$ on the system parameters $\{\tau_a, \tau_b, k_{\mathrm{on}}^{\mathrm{out}}, k_{\mathrm{off}}^{\mathrm{out}}\}$. With this perturbed matrix $\hat{\mathcal{A}}$, the steady-state covariance $\hat{\Sigma}_{X,\mathrm{ss}}$ satisfies a new Lyapunov equation

$$\hat{\Sigma}_{X,\mathrm{ss}}\mathcal{A} + \mathcal{A}^{\mathrm{T}}\hat{\Sigma}_{X,\mathrm{ss}} + \hat{\Sigma}_{X,\mathrm{ss}}\delta\mathcal{A} + \delta\mathcal{A}^{\mathrm{T}}\hat{\Sigma}_{X,\mathrm{ss}} + 2\mathcal{B}\Sigma_w\mathcal{B}^{\mathrm{T}} = 0.$$

Suppose that $\mathcal{A}$ is Hurwitz stable and $(\mathcal{A}, \mathcal{B})$ is controllable. If the perturbation $\delta\mathcal{A}$ is Hurwitz stable then $\hat{\Sigma}_{X,\mathrm{ss}} \geq \Sigma_{X,\mathrm{ss}}$, and if the perturbation $\delta\mathcal{A}$ is anti-Hurwitz stable (i.e., $-\delta\mathcal{A}$ is Hurwitz stable) then $\hat{\Sigma}_{X,\mathrm{ss}} \leq \Sigma_{X,\mathrm{ss}}$.[4] More specifically, consider a parametric perturbation $\hat{\theta} = \theta + \delta\theta$ for $\theta \in \{\tau_a, \tau_b, k_{\mathrm{on}}^{\mathrm{out}}, k_{\mathrm{off}}^{\mathrm{out}}\}$ in the matrix $\mathcal{A}$. The positive perturbation $\delta\theta > 0$ gives $\hat{\Sigma}_{X,\mathrm{ss}} \geq \Sigma_{X,\mathrm{ss}}$ and the negative perturbation $\delta\theta < 0$ gives $\hat{\Sigma}_{X,\mathrm{ss}} \leq \Sigma_{X,\mathrm{ss}}$ for any $\theta \in \{\tau_a, \tau_b, k_{\mathrm{on}}^{\mathrm{out}}, k_{\mathrm{off}}^{\mathrm{out}}\}$, provided $\theta, \hat{\theta} > 0$. In conclusion, the variation of the system output (or state) is a nondecreasing function of the system parameters $\{\tau_a, \tau_b, k_{\mathrm{on}}^{\mathrm{out}}, k_{\mathrm{off}}^{\mathrm{out}}\}$. This result is consistent with an intuition from the system dynamics, since, roughly speaking, those system parameters are linearly proportional to the inverse of the time constants.

5. System performance and sensitivity analysis using linearization

This section considers the analysis of the sensitivity of certain parameters to functionalities of the biological system. Similar to Section 4, the linearized model (5) of the motif dynamics (1) is used to facilitate sensitivity analysis.

5.1. $\mathcal{H}_\infty$ performance and sensitivity analysis

Observe that the system realization $(\mathcal{A}, \mathcal{B}, \mathcal{C})$ is a positive system in which $\mathcal{A}$ is a Metzler matrix, and $\mathcal{B}$ and $\mathcal{C}$ are nonnegative matrices, provided that all of the system parameters are positive. Computation of the $\mathcal{H}_\infty$ performance for this type of system can be performed without any frequency-dependent computation or solving a linear matrix inequality corresponding to the Kalman–Yakubovich–Popov Lemma. In particular, [30] shows that, for any scalar transfer function $G(s) = \mathcal{D} + \mathcal{C}(s\mathrm{I} - \mathcal{A})^{-1}\mathcal{B}$ with a positive realization $(\mathcal{A}, \mathcal{B}, \mathcal{C}, \mathcal{D})$,

$$\|G\|_\infty = \mathcal{D} - \mathcal{C}\mathcal{A}^{-1}\mathcal{B},$$

which is the steady-state gain of the system transfer function $G(s)$. More generally, for any square transfer function $G(s) = \mathcal{D} + \mathcal{C}(s\mathrm{I} - \mathcal{A})^{-1}\mathcal{B}$ with a positive realization $(\mathcal{A}, \mathcal{B}, \mathcal{C}, \mathcal{D})$,

$$\|G\|_\infty = \overline{\sigma}(\mathcal{D} - \mathcal{C}\mathcal{A}^{-1}\mathcal{B}),$$

which is the steady-state gain of the system transfer function $G(s)$, computed in terms of the induced 2-norm or the Euclidean norm for $\mathbb{R}^n$. For the linearized system (5), an analytical expression can be derived for the $\mathcal{H}_\infty$-norm of the system:

$$\|G\|_\infty = \frac{(1/\tau_a + 1/\tau_b)h(y)(1-y)(1-x)}{2h'(y)(1-y)(1-x)u - \left(2x + \frac{k_{\mathrm{off}}^{\mathrm{out}}}{k_{\mathrm{on}}^{\mathrm{out}}}\right)(1+h(y)u)}. \tag{8}$$

This closed-form expression can be used to study the sensitivity of the system performance with respect to the system parameters. For example, consider the case when $S_{\mathrm{ss}} = 1$ and a (deterministic) perturbation δS. A biased step perturbation $\delta S = \kappa \in \mathbb{R}$ in the stimulus will change the steady-state of the output by $\delta O_{\mathrm{ss}} = \kappa \| G \|_\infty$ so that the resultant output in the steady-state becomes $O_{\mathrm{ss}} + \delta O_{\mathrm{ss}}$. Thus, the closed-form expression (8) can be used to quantify the sensitivity of the output in the steady-state with respect to the system parameters of interest, as well as to study qualitative behavior of the system performance in terms of the $\mathcal{L}_2$-gain (or $\mathcal{H}_\infty$-norm).

[4] This is a property of Lyapunov equation; see ([29], Prop. 4.4) for details.

5.2. $\mathcal{H}_2$ performance and sensitivity analysis

Another commonly used system performance criterion is the $\mathcal{H}_2$-norm of a system transfer function. Computation of the $\mathcal{H}_2$ performance of a linear time-invariant system is relatively easy in the sense that only a linear programming problem needs to be solved. For a strictly proper transfer function $G(s) = \mathcal{C}(s\mathrm{I} - \mathcal{A})^{-1}\mathcal{B}$,

$$\|G\|_2 = \mathrm{Tr}(\mathcal{B}^{\mathrm{T}} Y_o \mathcal{B}),$$

where Y_o is the observability Gramian

$$Y_o = \int_0^\infty e^{\mathcal{A}^{\mathrm{T}} t} \mathcal{C}^{\mathrm{T}} \mathcal{C} e^{\mathcal{A}t} dt.$$

This observability Gramian is a unique solution for the Lyapunov equation $Y_o\mathcal{A} + \mathcal{A}^{\mathrm{T}} Y_o + \mathcal{C}^{\mathrm{T}}\mathcal{C} = 0$, provided that $\mathcal{A}$ is Hurwitz stable and the pair $(\mathcal{A}, \mathcal{C})$ is observable. Similar to the $\mathcal{H}_\infty$-norm computation, a closed-form analytical expression for $\|G\|_2$ with a realization (5) can be derived (not shown here due to space constraints). However, the closed-form solution has a somewhat complex dependence on the system parameters and it is hard to gain much intuition from the expression. This observation motivates a different approach that is similar to the noise sensitivity analysis in Section 4.3, in which a Lyapunov equation is used to study how the Lyapunov solution changes as a system parameter changes. Suppose that $\mathcal{A}$ is Hurwitz stable and $(\mathcal{A}, \mathcal{C})$ is observable. Consider a parametric perturbation $\delta\mathcal{A}$ with which the new system matrix is given by $\hat{\mathcal{A}} := \mathcal{A} + \delta\mathcal{A}$ and the corresponding system transfer function is defined by $\hat{G}(s) := \mathcal{C}(s\mathrm{I} - \hat{\mathcal{A}})^{-1}\mathcal{B}$. If the perturbation $\delta\mathcal{A}$ is Hurwitz stable then $\hat{Y}_o \geq Y_o$, which implies $\|\hat{G}\|_2 \geq \|G\|_2$, and if the perturbation $\delta\mathcal{A}$ is anti-Hurwitz stable (i.e., $-\delta\mathcal{A}$ is Hurwitz stable) then $\hat{Y}_o \leq Y_o$, which implies $\|\hat{G}\|_2 \leq \|G\|_2$. More specifically, consider a parametric perturbation $\hat{\theta} = \theta + \delta\theta$ for $\theta \in \{\tau_a, \tau_b, k_{\mathrm{on}}^{\mathrm{out}}, k_{\mathrm{off}}^{\mathrm{out}}\}$ in the matrix $\mathcal{A}$. The positive perturbation $\delta\theta \geq 0$ gives $\|\hat{G}\|_2 \geq \|G\|_2$ and the negative perturbation $\delta\theta \leq 0$ gives $\|\hat{G}\|_2 \leq \|G\|_2$ for any $\theta \in \{\tau_a, \tau_b, k_{\mathrm{on}}^{\mathrm{out}}, k_{\mathrm{off}}^{\mathrm{out}}\}$, provided $\theta, \hat{\theta} > 0$. The $\mathcal{H}_2$-norm can be used for a measure of performance when information is available on the spectral content of the input source and can be interpreted as (a) the output variance for a stationary stochastic noise applied at the input, (b) the system output energy variance for the impulse input, and (c) the output variance in the $\mathcal{L}_\infty$ norm over time for an arbitrary input in the $\mathcal{L}_2$ space (see ([29], Sec. 6) for details on $\mathcal{H}_2$ control). Therefore, the result in this section tells us that those measures of output variation incurred by an input of known spectrum are monotonically nondecreasing functions in the system parameters $\theta \in \{\tau_a, \tau_b, k_{\mathrm{on}}^{\mathrm{out}}, k_{\mathrm{off}}^{\mathrm{out}}\}$ and can be used to tune such system parameters to achieve a desired $\mathcal{H}_2$ performance of the system in a straightforward way.

6. Discussion

6.1. Response time and noise sensitivity

Output responses to a noise-free and noisy stimulus signal are shown in Figs. 4 and 5. All three components O, A, and B approach stable steady states both when the stimulus is on and when the stimulus is off. When the stimulus is turned on, the initial activation is slow as the output O is low and the value of the Hill term is close to zero, which is apparent from the plot for the "Two Slow Loop" case. It is harder to observe from the "Two Fast Loop" case because the total transition time from one state to another is very short. The dynamics of the output O follows more closely the dynamics of the faster loop when the stimulus S is switched from off to on because the value of $1 - O$ decreases with time. On the other hand, when the stimulus is switched from on to off, the dynamics of the output O follows more closely the dynamics of the slow loop as the value of $1 - O$ decreases with time. When the fast and the slow loop are coupled together, Fig. 4 shows that the system has fast response when turning on and slow response when turning off. A closer look in Fig. 6 shows the output response trajectories during the activation

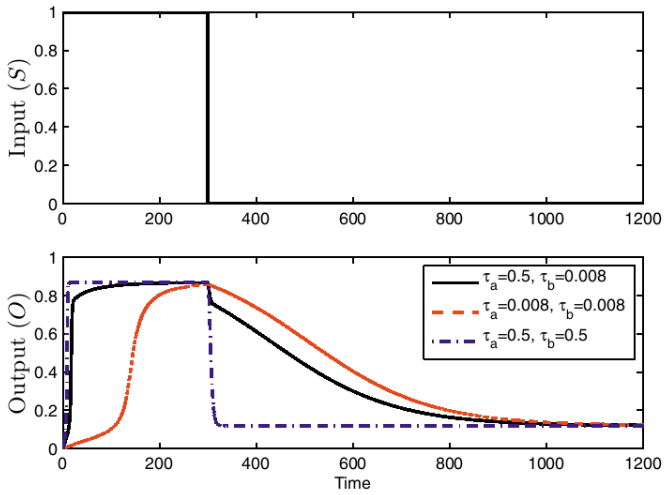

Fig. 4. Output trajectories for a pulse input for models with different time constants.

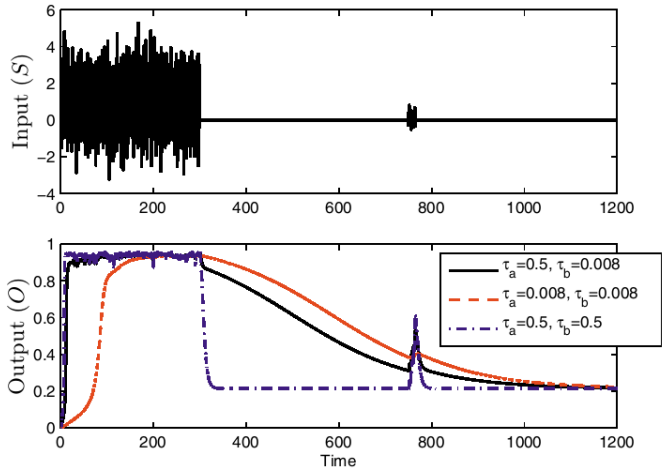

Fig. 5. Output trajectories for a pulse input for models with different time constants in the presence of additive noise in the stimulus.

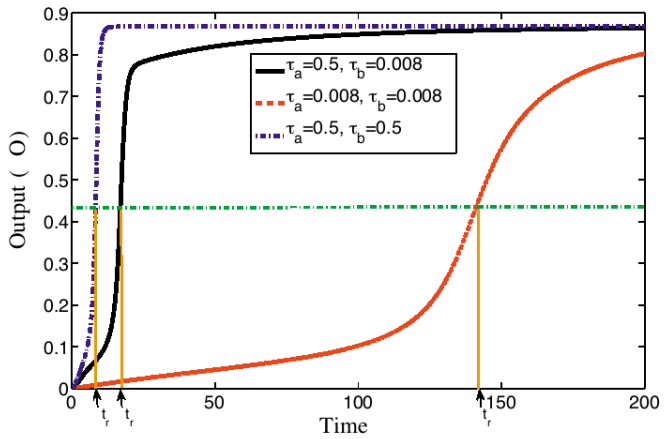

Fig. 6. A comparison of the response time (t_r) for models with different time constants.

by the step stimulus without noise. The response time denoted by t_r that is time when the output reaches half of the steady-state is compared for the models with different time constants. The response time of the dual-positive feedback loop case is twice as much as the one of the "Two Fast Loop" case, but almost nine times faster than the one of the "Slow Fast Loop" case. According to Fig. 5, where a pulse noise is applied during the transition from the on state to the off state, the output O is resistant to noise in the on state in the transition to the off state, compared to the "Two Fast Loop" case.

6.2. Approximate upper bounds on the loop states and output response: a Lyapunov method

Here a Lyapunov method is shown to provide a way to compute approximate upper bounds (or envelopes) on the loop states and output response when constant step inputs are applied. For notational convenience, the mathematical model for the dual-positive feedback loops motif can be written as

$$\begin{aligned}\dot{x}_1 &= \theta_1(x_2+x_3)(1-x_1)-\theta_2 x_1+\theta_3\\ \dot{x}_2 &= \theta_6\left(u\frac{x_1^3}{x_1^3+\theta_4^3}(1-x_2)-x_2+\theta_5\right) \qquad (9)\\ \dot{x}_3 &= \theta_7\left(u\frac{x_1^3}{x_1^3+\theta_4^3}(1-x_3)-x_3+\theta_5\right) \qquad (10)\\ y &= x_1,\end{aligned}$$

where u is the stimulus, y is the output response of the motif, and the states x_1 and x_2 correspond to the fast and slow loop, respectively.

Define an auxiliary input signal as

$$\nu \triangleq \frac{x_1^3}{x_1^3+\theta_4^3}u, \qquad (11)$$

and assume that the stimulus is bounded:

$$0 \le u \le u_{\max}. \qquad (12)$$

Since all system parameters in (9) are assumed to be positive, all the states are positive for all time and the auxiliary input ν is bounded as

$$0 \le \nu \le u_{\max}. \qquad (13)$$

Now consider the Lyapunov function

$$V_{23}(x_2,x_3) = \max\left\{x_2^2, x_3^2\right\}. \qquad (14)$$

Its upper right Dini derivative [31] at t in the direction ν, defined as

$$\overline{D^+}V_{23}(t,x;\nu) \triangleq \limsup_{h\to 0^+}\frac{V_{23}(t+h,x+h\nu)-V_{23}(t,x)}{h},$$

is less than or equal to zero for any $\nu \in \{\dot{x}_2, \dot{x}_3\}$ whenever

$$(x_2,x_3) \in \left\{(x,y)\in\mathbb{R}_+^2 | x \ge \frac{\theta_5+\nu}{1+\nu} \quad \text{or} \quad y \ge \frac{\theta_5+\nu}{1+\nu}\right\}, \qquad (15)$$

which follows from results in [32,33]. This implies that the solutions of (9) are ultimately bounded and the output (10) is also bounded:

$$y = x_1 \le \max\left\{\frac{\theta_3}{\theta_2}, \frac{\theta_3+2\theta_1\xi_{23,\max}}{\theta_2+2\theta_1\xi_{23,\max}}\right\} =: y_{bd}^{u_{\max}} \qquad (16)$$

$$x_k \le \xi_{23,\max} =: x_{k,\mathrm{bd}}^{u_{\max}} \quad \text{for } k=2,3 \qquad (17)$$

with

$$\xi_{23,\max} \triangleq \max\left\{\theta_5, \frac{\theta_5+u_{\max}}{1+u_{\max}}\right\}, \qquad (18)$$

provided that the initial states x_{10}, x_{20}, and x_{30} of the solution in (9) start from the inside of the above bounds. It is not difficult to see that, if the stimulus presented in the motif is a step function, then the above upper bounds give proper approximations of the steady-state values. In other words, $y_{\mathrm{ss}}^{0D} = y_{\mathrm{bd}}^{(u_{\max}=0)}$ and $y_{\mathrm{ss}}^{1D} = y_{\mathrm{bd}}^{(u_{\max}=1)}$. This analysis of Lyapunov method provides analytical relations between the parameters $\{\theta_1, \theta_2, \theta_3, \theta_5\}$ and the steady-states (or the maximum values of states). Such relations can be also used for manipulating system parameters to achieve desired system behaviors.

7. Conclusion

This paper details the analysis of model equations describing the dual-positive feedback loops that regulate the gene switches in many biological systems. It is described how model parameters can be estimated from experimental data, for different choices of measured variables. Relating the kinetic parameters with the dynamic behaviors, system performance, and sensitivity of the binary switches can enable the prediction of the behavior of regulatory networks that could be used to facilitate the design of gene switches to achieve desired behaviors.

References

[1] S. Bornholdt, Systems biology: less is more in modeling genetic networks, Science 310 (2005) 449–451.
[2] O. Brandman, J.E. Ferrett Jr., R. Li, T. Meyer, Interlinked fast and slow positive feedback loops drive reliable cell decisions, Science 310 (2005) 496–498.
[3] J.C.W. Locke, P.O. Westermark, A. Kramer, H. Herzel, Global parameter search reveals design principles of the mammalian circadian clock, BMC Systems Biology 2 (2008), art no. 22.
[4] F. Li, T. Long, Y. Lu, Q. Ouyang, C. Tang, The yeast cell-cycle network is robustly designed, Proceedings of National Academy of Sciences of United States of America 101 (2004) 4781–4786.
[5] S. Hildebrandt, D. Raden, L. Petzold, A.S. Robinson, F.J. Doyle III, A top-down approach to mechanistic biological modeling: application to the single-chain antibody folding pathway, Biophysical Journal 95 (2008) 3535–3558.
[6] M. Nykter, N.D. Price, M. Aldana, S.A. Ramsey, S.A. Kauffman, L.E. Hood, O. Yli-Harja, I. Shmulevich, Gene expression dynamics in the macrophage exhibit criticality, Proceedings of National Academy of Sciences of United States of America 105 (2008) 1897–1900.
[7] O. Brandman, T. Meyer, Feedback loops shape cellular signals in space and time, Science 322 (2008) 390–395.
[8] K. Horikawa, K. Ishimatsu, E. Yoshimoto, S. Kondo, H. Takeda, Noise-resistant and synchronized oscillation of the segmentation clock, Nature 441 (2006) 719–723.
[9] J. Lewis, Autoinhibition with transcriptional delay: a simple mechanism for the zebrafish somitogenesis oscillator, Current Biology 13 (2003) 1398–1408.
[10] A.L. Barabasi, Z.N. Oltvai, Network biology: understanding the cells functional organization, Nature Reviews Genetics 5 (2004) 101–113.
[11] T.I. Lee, N.J. Rinaldi, F. Robert, D.T. Odom, Z. Bar-Joseph, G.K. Gerber, N.M. Hannett, C.T. Harbison, C.M. Thompson, I. Simon, J. Zeitlinger, E.G. Jennings, H.L. Murray, D.B. Gordon, B. Ren, J.J. Wyrick, J.B. Tagne, T.L. Volkert, E. Fraenkel, D. Gifford, R. Young, Transcriptional regulatory networks in *Saccharomyces cerevisiae*, Science 298 (2002) 799–804.
[12] O. Sporns, R. Kotter, Motifs in brain networks, PLoS Biology 2 (2004) 1910–1918.
[13] R. Milo, S. Shen-Orr, S. Itzkovitz, N. Kashtan, D. Chklovskii, U. Alon, Network motifs: simple building blocks of complex networks, Science 298 (2002) 824–827.
[14] R.J. Prill, P.A. Iglesias, A. Levchenko, Dynamic properties of network motifs contribute to biological network organization, PLoS Biology 3 (2005) 1881–1892.
[15] S.S. Shen-Orr, R. Milo, S. Mangan, U. Alon, Network motifs in the transcriptional regulation network of *Escherichia coli*, Nature Genetics 31 (2002) 64–68.
[16] D.M. Wolf, A.P. Arkin, Motifs, modules and games in bacteria, Current Opinion in Microbiology 6 (2003) 125–134.
[17] R. McDaniel, R. Weiss, Advances in synthetic biology: on the path from prototypes to applications, Current Opinion in Biotechnology 16 (2005) 476–483.
[18] T. Gardner, C.R. Cantor, J.J. Collins, Construction of a genetic toggle switch in *Escherichia coli*, Nature 403 (2000) 339–342.

[19] H. Kobayashi, M. Kaern, M. Araki, K. Chung, T.S. Gardner, C.R. Cantor, J.J. Collins, Programmable cells: interfacing natural and engineered gene networks, Proceedings of National Academy of Sciences of United States of America 101 (2004) 8414–8419.
[20] M.R. Atkinson, M.A. Savageau, J.T. Myers, A.J. Ninfa, Development of genetic circuitry exhibiting toggle switch or oscillatory behavior in *Escherichia coli*, Cell 113 (2003) 597–607.
[21] J. Stricker, S. Cookson, M.R. Bennett, W.H. Mather, L.S. Tsimring, J. Hasty, A fast, robust and tunable synthetic gene oscillator, Nature 456 (2008) 516–519.
[22] M.B. Elowitz, S. Leibler, A synthetic oscillatory network of transcriptional regulators, Nature 403 (2000) 335–338.
[23] E. Fung, W.W. Wong, J.K. Suen, S.G.L.T. Bulter, J.C. Liao, A synthetic gene-metabolic oscillator, Nature 435 (2005) 118–122.
[24] L.C. You, R.S. Cox, R. Weiss, F.H. Arnold, Programmed population control by cell–cell communication and regulated killing, Nature 428 (2004) 868–871.
[25] M. Savageau, Design principles for elementary gene circuits: elements, methods, and examples, Chaos 11 (2001) 142–159.
[26] H.K. Khalil, Nonlinear Systems, Prentice Hall, Upper Saddle River, NJ, 2002.
[27] H. El Samad, M. Khammash, Stochastic stability and its application to the analysis of gene regulatory networks, in: Proceedings of the IEEE Conference on Decision and Control, San Diego, CA, 2004, pp. 3001–3006.
[28] A. Lasota, M.C. Mackey, Chaos, Fractals and Noise: Stochastic Aspects of Dynamics, Springer, New York, 1994.
[29] G.E. Dullerud, F. Paganini, A Course in Robust Control Theory: A Convex Approach, Springer, New York, 2000.
[30] A. Rantzer, Distributed control of positive systems, in: Proceedings of the IEEE Conference on Decision and Control, Orlando, FL, 2011, pp. 6608–6611.
[31] A.F. Filippov, Differential Equations with Discontinuous Righthand Sides, Springer, Dordrecht, Netherlands, 1988.
[32] E. Sontag, H.J. Sussmann, Nonsmooth control-Lyapunov functions, in: Proceedings of the IEEE Conference on Decision and Control, New Orleans, LA, 1995, pp. 2799–2805.
[33] A. Bacciotti, F. Ceragioli, Stability and stabilization of discontinuous systems and nonsmooth Lyapunov functions, control, Optimization and Calculus of Variations 4 (1999) 361–376.